

# Robust Design Optimization of a Permanent Magnet Motor from the System-Level Design Perspective

Jaegyong Mun<sup>1</sup>, K. K. Choi<sup>2</sup>, and Dong-Hun Kim<sup>1\*</sup>

<sup>1</sup>*Dept. of Electrical Eng., Kyungpook National Univ., Daegu 41566, Republic of Korea*

<sup>2</sup>*Dept. of Mechanical and Industrial Eng., Univ. of Iowa, Iowa City, IA 52242-1527, USA*

(Received 7 March 2022, Received in final form 13 March 2022, Accepted 13 March 2022)

**From the system-level design perspective, a robust design optimization method for a permanent magnetic motor is proposed to enhance the dynamic performance of a drive system while maintaining its steady performance. To achieve the goal, an elaborate numerical model for the whole drive system is first constructed by incorporating a control circuit simulator into a finite element analysis tool, and then the influence of motor parameter variations on transient system responses is investigated by means of the method of Taguchi experimental planning. A conventionally customized motor is optimized by the univariate dimension reduction method to ensure the robustness of system performances against manufacturing tolerances. Finally, a comparative performance analysis between two motor drive systems is provided to demonstrate the validity of the proposed method.**

**Keywords :** electromagnetics, optimization, reliability theory, robustness

## 1. Introduction

A motor drive system consisting of a permanent magnet motor, inverter/converter, and controller has drawn great attention from engineers as it is playing an important role in modern home and industrial appliances. In developing such a drive system, engineers easily encounter a very tricky but very important subject on how to find the most insensitive system design to uncontrollable design factors while enhancing or maintaining dynamic and steady system performances. To manage this complicated issue, various attempts have been made in academic and industrial communities so far.

To handle the electromagnetic (EM) product quality, several approaches such as the worst-case scenario, Taguchi quality design, and Monte Carlo simulation (MCS) have been widely used in an early design stage [1-3]. However, the first two methods do not address the quantitative assessment of the first two statistical moments, mean and variance, of system performances. In other words, they cannot give accurate probabilistic information on how much the impact of the uncertainty concerned with

system inputs is on system outputs at a given EM design [4-7]. On the other hand, MCS could be accurate for the moment estimation, but it requires a large number of function evaluations. Therefore, it is not practical that MCS is applied to the robust design optimization (RDO) of EM appliances, especially with multi-dimensional design variables. To overcome the shortcomings of three RDO methods, a univariate dimension reduction method (DRM) was recently proposed [5, 7]. Therein any n-dimensional performance function was additively decomposed into one-dimension ones, and its numerical accuracy and efficiency were tested through optimizing a permanent magnet motor alone. When the individually optimized motor is assembled into a drive system, however, it cannot necessarily guarantee the best performance of the holistic system. The component-level system design methods of this kind may not ensure that a whole system is robust with respect to design requirements when exposed to the variation of system parameters.

In the meanwhile, through a lot of empirical experience in dealing with EM-related systems, it has been widely recognized that when designing an electrical system, the so-called system-level design optimization should be necessarily required. Under this integrated design scheme, the cooperative relationships between system components must be investigated simultaneously, and then a multi-

---

©The Korean Magnetism Society. All rights reserved.

\*Corresponding author: Tel: +82-53-950-5603

Fax: 82-53-950-5600, e-mail: dh29kim@ee.knu.ac.kr

domain design optimization problem including physical phenomena linked to the system must be solved accurately [8-10]. Therefore, it is a very difficult task for system designers, but it will be very worth challenging work. In order to tackle the design problem of a motor drive system, a few studies have been conducted in recent years [9, 10]. In both two articles, a permanent magnet motor was optimized by means of the Taguchi quality design method from the system-level design point of view. However, the method is apt to yield very erroneous numerical results because it cannot reflect the complexity of highly nonlinear performance functions. Moreover, it does not give any design sensitivity information of statistical moments, and it may often lead to an unaffordable computing cost to seek an optimum especially when multidimensional design variables are dealt with.

As an effort to realize more robust and better performances of a motor drive system in the presence of manufacturing tolerances, this paper makes an attempt to develop a design methodology of system-level robust optimization based on the univariate DRM and highly elaborate motor system simulator.

## 2. System Simulator and Parameter Investigation

In this chapter, a numerical simulator to accurately predict dynamic and steady performances of a motor drive system is first described, and the effect of motor parameters on transient system responses is then examined by means of the method of Taguchi experimental planning.

### 2.1. Motor Drive Simulator

A 3-phase, 4-pole, 24-slot, 700 W, interior-type permanent magnet synchronous motor with a drive controller is considered. To estimate drive system responses, a commercial finite element analysis (FEA) tool called MagNet is interlocked with a drive control simulator of MATLAB/Simulink [11, 12]. As seen in Fig. 1, the motor operates from a standstill to the rated speed of 1,800 rpm based on the field-oriented control (FOC) law where the rotating direct-quadrature ( $d-q$ ) reference frame is synchronized with the rotor magnet. Utilizing a feedback technique based on the proportional-integral compensator for the exceedance of armature voltage, the control system can achieve optimal control through the speed and current controllers. For the sake of simplicity, inverter and converter units are omitted in the presented block diagram.

As for the test motor, four neodymium (NdFeB) permanent magnets with a width of 22.83 mm and a height of 1.22 mm are inserted in the rotor. The stator has inner and outer diameters of 56.5 and 112 mm, respectively. The core stacking length is 65 mm, and the airgap length is 0.5 mm. The armature winding consists of 140 turns per coil and two coils in series per phase per pole. A cross-section of the motor is discretized into triangle finite elements with the second-order interpolation functions, and accordingly magnetic field simulation is executed by the nonlinear transient FEA solver with motion where the phase voltage is supplied from the drive controller. Fig. 2 illustrates the distribution of magnetic flux density on the FEA motor model obtained at a certain rotor position under a full load condition.

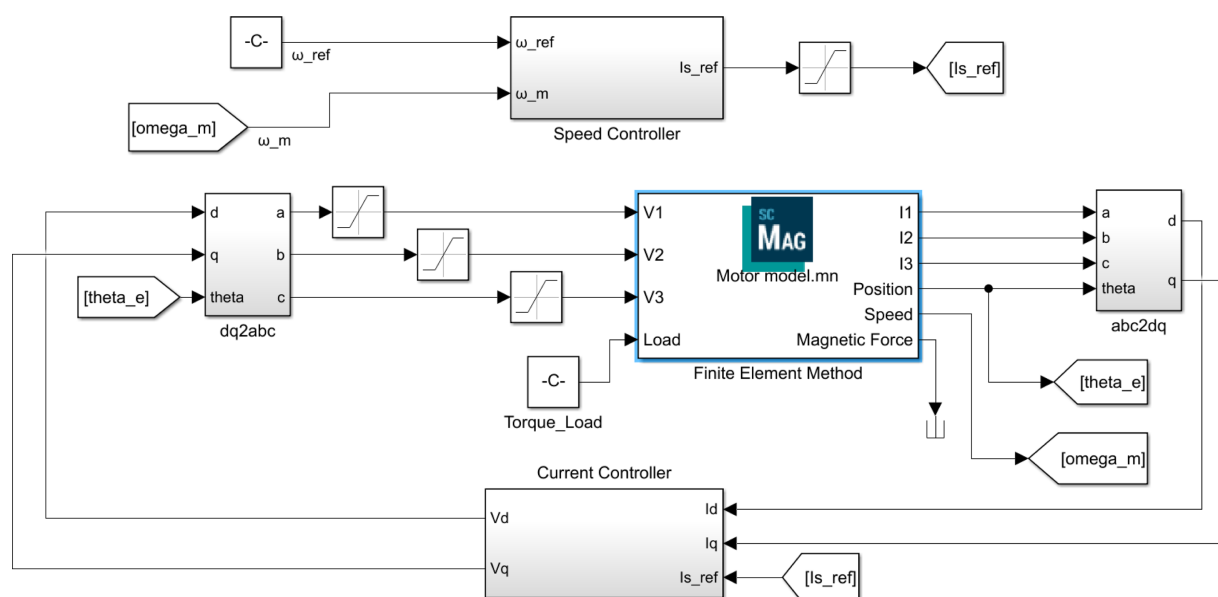
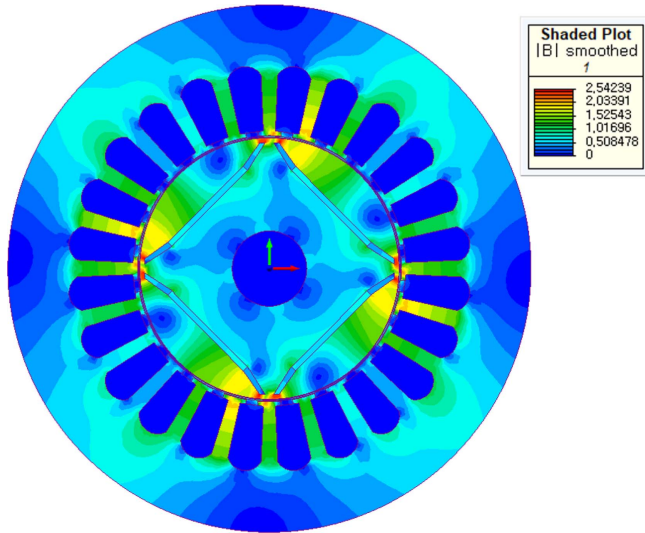


Fig. 1. (Color online) Block diagram of a motor drive system based on the FOC in  $d-q$  frame.



**Fig. 2.** (Color online) Magnetic flux density distribution on a cross section of the motor.

**2.2. Motor Parameter Investigation**

In most cases of control algorithms, a mathematical model in the *d-q* reference frame is used so that the speed and torque of a motor can be precisely adjusted by exploiting motor parameter values estimated for winding resistance and inductance in advance [13]. In a mass-production system, however, the motor parameters are not always constant. Especially when compared to the winding resistance, due to the manufacturing tolerance, there exists a relatively considerable difference in inductance values between even the same-specification products. Therefore, the investigation on a comprehensive relationship between *d-q* axis inductances and controllers is an essential prerequisite to ensuring the robustness of motor drive systems.

In order to quantitatively assess the influence of individual inductances on dynamic system performances, a standard orthogonal array L4 was selected here for the matrix numerical experiments as shown in Table 1. In this array, the *d*-axis and *q*-axis inductances,  $L_d$  and  $L_q$ , were given as two control factors with two levels, of which the value

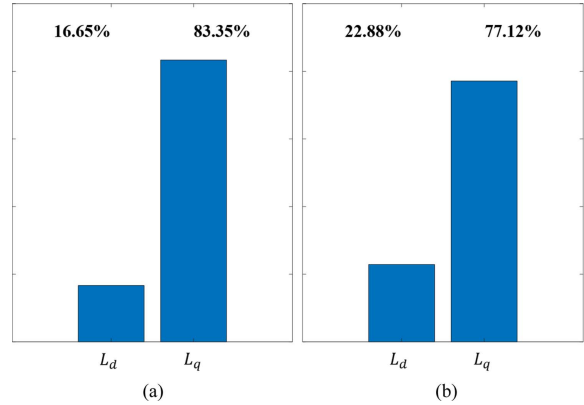


**Fig. 3.** (Color online) Percentage contribution of control factors on response: (a) overshoot, (b) settling time.

was defined from the standard deviation ( $\sigma$ ) of each inductance. Two transient system responses for the four combinations, variations of overshoot (OS) and settling time ( $t_s$ ), were examined where  $t_s$  was set to the time required for the speed response curve to reach and stay within a range of 2 % of the rated speed.

Based on the motor simulator presented in Fig. 1, statistical moment values in Table 1 were evaluated with the help of the univariate DRM under a certain disturbance of motor design variables (refer to Fig. 4 and Table 2). Fig. 3 shows the percentage contribution (PC) of each axis inductance on two kinds of system responses. It is observed the PC value of  $L_q$  is almost 4 times larger than that of  $L_d$  in both cases considered. This means that the *q*-axis inductance gives the biggest contribution to affecting dynamic system responses compared to the other factor. From the above result, it can be inferred that managing the variation of  $L_q$  due to the manufacturing tolerance is the best choice to obtain a robust and optimal motor design in terms of overall system performance.

**3. Case Study: Interior-Type Permanent Magnet Synchronous Motor**

To verify the validity of the proposed system-level

**Table 1.** L4(2<sup>3</sup>) Orthogonal Array for Two Factors with Two Levels and Their Responses.

No. of experiments	Factor	$L_d$	$L_q$	Responses	
	Level	$\sigma_{L_d}$ $2\sigma_{L_d}$	$\sigma_{L_q}$ $2\sigma_{L_q}$	Variance of OS	Variance of $t_s$
1		$\sigma_{L_d}$	$\sigma_{L_q}$	$4.92 \times 10^{-4}$	$2.79 \times 10^{-8}$
2		$\sigma_{L_d}$	$2\sigma_{L_q}$	$1.77 \times 10^{-3}$	$9.49 \times 10^{-8}$
3		$2\sigma_{L_d}$	$\sigma_{L_q}$	$7.01 \times 10^{-4}$	$4.47 \times 10^{-8}$
4		$2\sigma_{L_d}$	$2\sigma_{L_q}$	$1.98 \times 10^{-3}$	$1.12 \times 10^{-7}$

The values,  $\sigma_{L_d}$  and  $\sigma_{L_q}$ , of the test motor were calculated as  $5.39 \times 10^{-4}$  and  $9.53 \times 10^{-4}$ , respectively.

robust design optimization method, the conventionally customized motor is optimized by using the FEA-based motor simulator in conjunction with the univariate DRM technique. Then, a close investigation on dynamic and steady system performances between two different motor designs is made.

### 3.1. Optimization Problem Formulation

The design goal is to find the most insensitive motor design to the unavoidable manufacturing tolerances occurring in design variables while improving the overshoot and settling time of the drive system as well as retaining an average torque and cogging torque of the test most. For the purpose of managing somewhat complicated requirements, the  $q$ -axis inductance is defined as a target performance function  $h$  in the proposed RDO formulation of (1). According to the parameter survey results, the variance ( $\sigma_h^2$ ) of  $h$  is set to be minimized as a cost function ( $f$ ). Two constraint conditions on the cogging torque ( $T_c$ ) and average torque ( $T_{avg}$ ) at the rated speed of 1,800 rpm are additionally imposed as follows:

$$\begin{aligned} & \text{minimize } f = \sigma_h^2 / \sigma_{h0}^2, \quad h = L_q(\mathbf{x}; \mathbf{d}), \quad \mathbf{d} = \mu(\mathbf{x}) \\ & \text{subject to } T_c(\mathbf{x}; \mathbf{d}) \leq 0.17, \quad T_{avg}(\mathbf{x}; \mathbf{d}) \geq 3.67 \end{aligned} \quad (1)$$

where  $\sigma_{h0}$  is the nominal value of standard deviation (SD) of  $h$  which is calculated for the initial motor,  $\mathbf{x}$  is the random design variable vector, and  $\mathbf{d}$  is the design variable vector given by the mean ( $\mu$ ) of  $\mathbf{x}$ .

In order to alleviate a heavy burden on nonlinear transient FEA computations of the whole motor system, a quarter motor model as seen in Fig. 4 is considered here.

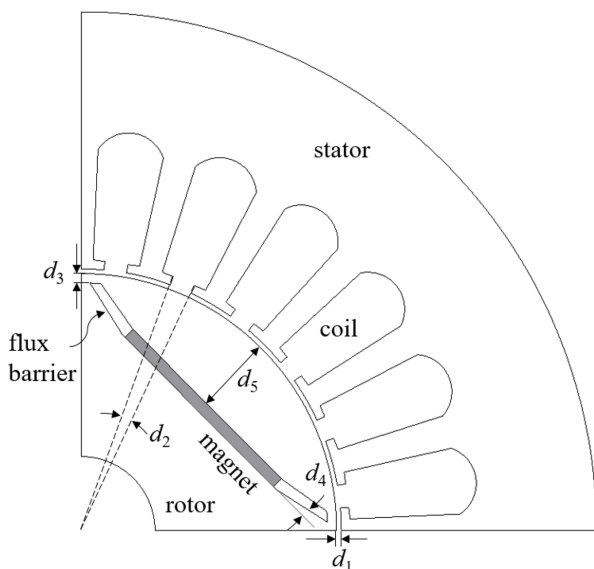


Fig. 4. A quarter motor model and design variables.

Table 2. Properties of Random Design Variables.

Variable	Unit	$x^L$	$x^U$	SD
$x_1$	mm	0.4	0.6	0.01
$x_2$	deg.	4.5	7.0	0.1
$x_3$	mm	0.5	1.5	0.1
$x_4$	deg.	10.0	15.0	0.1
$x_5$	mm	7.0	8.5	0.1

The motor geometry is characterized by five main design variables as in Fig. 4 where  $d_1$ ,  $d_2$ ,  $d_3$ ,  $d_4$ , and  $d_5$  correspond to the airgap length, angle of a slop opening, rib thickness, angle of a flux barrier, and magnet depth from the rotor surface, respectively. The random design variables are assumed to comply with Gaussian normal probability distributions, and their SD values are presented in Table 2 where the symbols,  $x^L$  and  $x^U$ , denote the lower and upper bounds of each random variable, respectively. The main optimization program was implemented in MATLAB, of which a function call remotely executed MagNet and Simulink. Therein, the sequential quadratic programming algorithm was utilized for handling the constrained optimization problem of (1).

### 3.2. Result and Discussion

Launching at the initial motor design, the design problem of (1) was solved by means of the univariate DRM to accurately predict statistical moments of the target performance function and their design sensitivities [5, 7]. Performance indicators between two different motors are presented in Table 3, where at least more than 11 FEA simulator calls at each design point are required only for obtaining the statistical information of  $h$ . It is obvious that the cost function (i.e. variance of  $q$ -axis inductance) is selectively reduced to almost 25 % of the initial one,

Table 3. Performance Indicators between two different motor designs.

	Parameter	Initial	Optimized
Design variables	$d_1 = \mu(x_1)$	0.50	0.60
	$d_2 = \mu(x_2)$	5.00	4.56
	$d_3 = \mu(x_3)$	1.00	0.54
	$d_4 = \mu(x_4)$	12.66	12.92
	$d_5 = \mu(x_5)$	8.41	7.64
Performances	$f$	1.000	0.769
	$L_q$ (H)	0.100	0.094
	$T_c$ (Nm)	0.163	0.169
	$T_{avg}$ (Nm)	3.678	3.676
	Iterative designs	-	15
	FEA simulator calls	11	4697

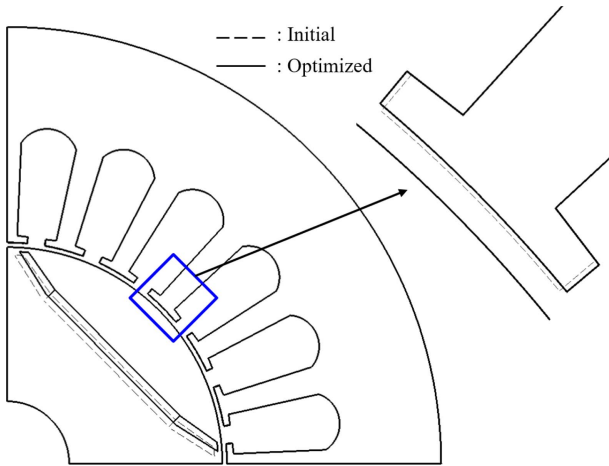


**Fig. 5.** (Color online) Outline comparison between two motor designs.

while satisfying the two constraints imposed on the cogging torque and average torque, respectively. The cross sections of the motors are compared with each other in Fig. 5 where the biggest change appears in the rib thickness ( $d_3$ ) and magnet depth ( $d_5$ ). It implies that steady motor performances are still maintained in both cases even though the two motors have a recognizable difference, especially in the rotor shape correlated with the magnet. It comes from the fact that when compared to the initial motor shape, the decreased rib thickness and magnet depth of the optimized one compensate for the decrease effect on the linkage flux and airgap flux density due to the increased airgap length ( $d_1$ ).

On the other hand, the probabilistic distributions of  $d$ - $q$  axis inductances caused by the manufacturing tolerances prescribed in In Table 2 are compared before and after

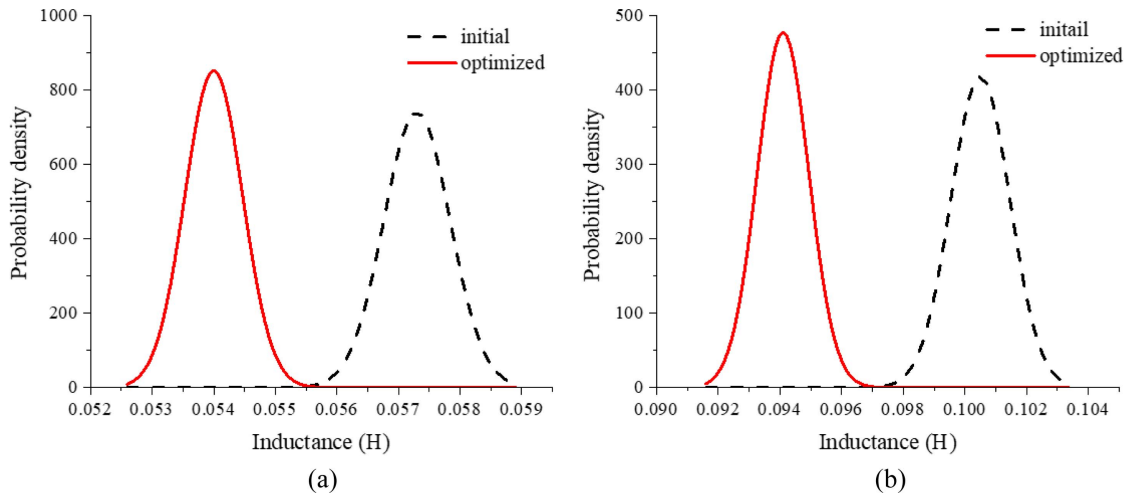


**Fig. 6.** (Color online) Probabilistic distributions of  $d$ - $q$  axis inductances due to the given manufacturing tolerances before and after optimization: (a)  $d$ -axis inductance, (b)  $q$ -axis inductance.

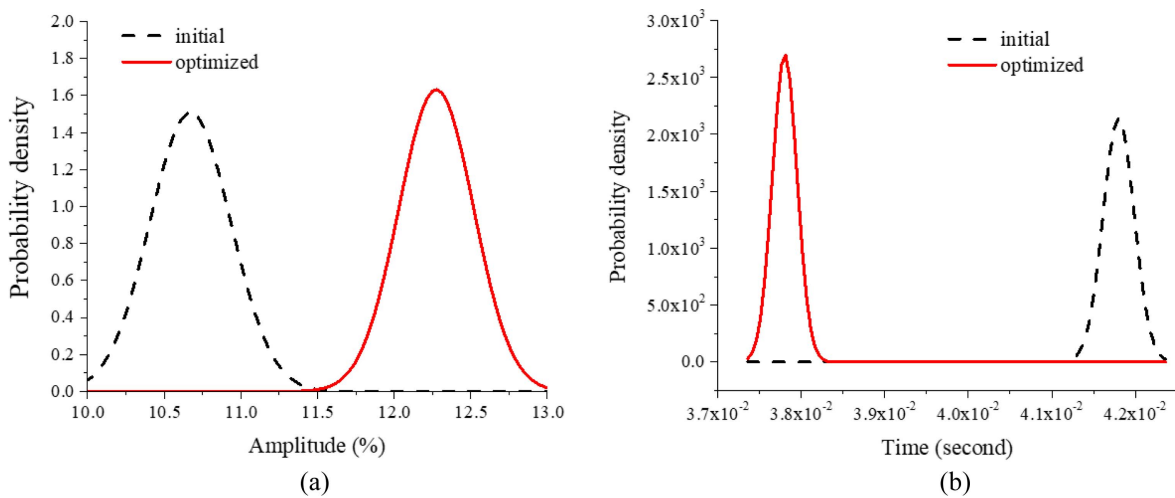


**Fig. 7.** (Color online) Probabilistic distributions of dynamic system responses due to the given manufacturing tolerances before and after optimization: (a) overshoot, (b) settling time.

optimization. The mean values of two inductances for the optimized motor become smaller by nearly 6 % with reference to their initial ones, whereas their variance values decrease almost up to 24 %. It shows that the optimized motor has much smaller variations in winding inductances under the same machining errors when compared to the initial one.

Finally, the variations of transient system responses between the two motors are measured in terms of overshoot and settling time, and accordingly their probabilistic distributions are presented in Fig. 7. As seen in Fig. 7(a), the mean of overshoot for the optimized motor is larger than the initial one by 15 %, but its variance value is decreased by 14.4 %. As for the settling time in Fig. 7(b), the mean and variance values of the optimized motor are reduced by more than 9.6 % and 37 %, respectively.

From the above comparison results, it can be deduced that the optimized motor is much more robust in dynamic system performances against the given manufacturing tolerances while its steady system performances are maintained.

#### 4. Conclusion

A robust design optimization method for a motor drive system is proposed through a thorough investigation between motor and controller parameters and a highly elaborate FEA-based simulator. Results show that the method can provide a good alternative to seeking a robust optimal design of electric motors from the system-level design perspective, especially when manufacturing tolerances are engaged in design variables.

#### Acknowledgment

This work was supported by the National Research Foundation of Korea (NRF) through the Basic Science Research Program funded by the Ministry of Education, Science and Technology under Grant 2019R1A2C1089638.

#### References

- [1] F. Guimaraes, D. Lowther, and J. Ramirez, *IEEE Trans. Magn.* **42**, 1207 (2006).
- [2] N. Kim, D. Kim, H. Kim, D. Lowther, and J. Sykulski, *IEEE Trans. Magn.* **46**, 3117 (2010).
- [3] X. Liu, S. Wang, J. Qiu, J. Zhu, Y. Guo, and Z. Lin, *IEEE Trans. Magn.* **44**, 978 (2008).
- [4] N. Sengil, *IEEE Trans. Plasma Sci.* **41**, 1156 (2013).
- [5] I. Lee, K. Choi, L. Du, and D. Gorsich, *J. Comput. & Struct.* **86**, 1550 (2007).
- [6] Y. H. Sung, D. Kim, and D. Kim, *IEEE Trans. Magn.* **47**, 4623 (2011).
- [7] D. Kim, N. Choi, C. Lee, and D. Kim, *IEEE Trans. Magn.* **51**, 7016804 (2015).
- [8] G. Lei, Y. G. Guo, J. G. Zhu, T. S. Wang, X. M. Chen, and K. R. Shao, *IEEE Trans. Magn.* **48**, 923 (2012).
- [9] G. Lei, T. Wang, Y. Guo, J. Zhu, and S. Wang, *IEEE Trans. Ind. Electron.* **61**, 6591 (2014).
- [10] G. Lei, T. Wang, J. Zhu, Y. Guo, and S. Wang, *IEEE Trans. Ind. Electron.* **62**, 4702 (2015).
- [11] *MagNet User's Manual*, Infolytica Corporation, Quebec, Canada, 2008.
- [12] *MATLAB/Simulink*, MathWorks, Massachusetts, USA, 2020.
- [13] Y. Inoue, S. Morimoto, and M. Sanada, *IEEE Trans. Ind. Appl.* **48**, 2382 (2012).